

## Research Paper

# Gastrin-releasing Peptide Receptor Imaging in Breast Cancer Using the Receptor Antagonist $^{68}\text{Ga}$ -RM2 And PET

Christian Stoykow<sup>1,4,5</sup>✉\*, Thalia Erbes<sup>2\*</sup>, Helmut R Maecke<sup>1,5</sup>, Stefan Bulla<sup>1</sup>, Mark Bartholomä<sup>1</sup>, Sebastian Mayer<sup>2</sup>, Vanessa Drendel<sup>3</sup>, Peter Bronsert<sup>3,5,8</sup>, Martin Werner<sup>3,5</sup>, Gerald Gitsch<sup>2</sup>, Wolfgang A Weber<sup>6</sup>, Elmar Stickeler<sup>7</sup>, Philipp T Meyer<sup>1,5</sup>

1. Department of Nuclear Medicine, Medical Center – University of Freiburg, Faculty of Medicine, University of Freiburg, Germany;
2. Department of Obstetrics and Gynecology, University Medical Center Freiburg, Germany;
3. Department of Clinical Pathology, University Medical Center Freiburg, Germany;
4. German Cancer Research Center (DKFZ), Heidelberg, Germany;
5. German Cancer Consortium (DKTK), Freiburg, Germany;
6. Molecular Imaging and Therapy Service, Department of Radiology, Memorial Sloan Kettering Cancer Center, New York, United States of America;
7. Department of Gynecology and Obstetrics, University Hospital Aachen, Germany;
8. Tumorbank, Comprehensive Cancer Center Freiburg, University Medical Center Freiburg, Germany.

\*Both authors contributed equally.

✉ Corresponding author: Christian Stoykow, Department of Nuclear Medicine, University Medical Center Freiburg, Hugstetter Str. 55, 79106, Freiburg, Tel.: +49-761-27074210; Fax: +49-761-27073500; eMail: christian.stoykow@uniklinik-freiburg.de.

© Ivyspring International Publisher. Reproduction is permitted for personal, noncommercial use, provided that the article is in whole, unmodified, and properly cited. See <http://ivyspring.com/terms> for terms and conditions.

Received: 2016.01.13; Accepted: 2016.04.08; Published: 2016.06.19

## Abstract

**Introduction:** The gastrin-releasing peptide receptor (GRPR) is overexpressed in breast cancer. The present study evaluates GRPR imaging as a novel imaging modality in breast cancer by employing positron emission tomography (PET) and the GRPR antagonist  $^{68}\text{Ga}$ -RM2.

**Methods:** Fifteen female patients with biopsy confirmed primary breast carcinoma (3 bilateral tumors; median clinical stage IIB) underwent  $^{68}\text{Ga}$ -RM2-PET/CT for pretreatment staging. *In vivo* tumor uptake of  $^{68}\text{Ga}$ -RM2 was correlated with estrogen (ER) and progesterone (PR) receptor expression, HER2/neu status and MIB-1 proliferation index in breast core biopsy specimens.

**Results:** 13/18 tumors demonstrated strongly increased  $^{68}\text{Ga}$ -RM2 uptake compared to normal breast tissue (defined as PET-positive). All PET-positive primary tumors were ER- and PR-positive (13/13) in contrast to only 1/5 PET-negative tumors. Mean  $\text{SUV}_{\text{MAX}}$  of ER-positive tumors was  $10.6 \pm 6.0$  compared to  $2.3 \pm 1.0$  in ER-negative tumors ( $p=0.016$ ). In a multivariate analysis including ER, PR, HER2/neu and MIB-1, only ER expression predicted  $^{68}\text{Ga}$ -RM2 uptake (model:  $r^2=0.55$ ,  $p=0.025$ ). Normal breast tissue showed inter- and intraindividually variable, moderate GRPR binding ( $\text{SUV}_{\text{MAX}}$   $2.3 \pm 1.0$ ), while physiological uptake of other organs was considerably less except pancreas. Of note,  $^{68}\text{Ga}$ -RM2-PET/CT detected internal mammary lymph nodes with high  $^{68}\text{Ga}$ -RM2 uptake ( $n=8$ ), a contralateral axillary lymph node metastasis (verified by biopsy) and bone metastases ( $n=1$ ; not detected by bone scan and CT).

**Conclusion:** Our study demonstrates that  $^{68}\text{Ga}$ -RM2-PET/CT is a promising imaging method in ER-positive breast cancer. *In vivo* GRPR binding assessed by  $^{68}\text{Ga}$ -RM2-PET/CT correlated with ER expression in primary tumors of untreated patients.

Key words: GRPR, gastrin-releasing peptide receptor, bombesin, PET, positron emission tomography, breast cancer, ER, estrogen receptor.

## Introduction

The gastrin-releasing peptide receptor (GRPR) is a promising target for molecular imaging and targeted therapy, showing an overexpression in several human tumors such as prostate carcinoma, breast cancer (BC), and peritumoral vessels in ovarian cancer [1, 2]. Using autoradiography Reubi et al found a GRPR expression of high density in 72-74 % of ductal BC specimens [2, 3], while Dalm et al. observed an even higher fraction of GRPR-positive samples of 96 % [4]. GRPR is a subtype of the bombesin receptor family with the physiologic ligand gastrin releasing peptide (GRP). GRP has various physiologic functions, including the release of gastrin and regulation of enteric motor function. GRP and GRPR also appear to play a (so far poorly characterized) role in human carcinogenesis and tumor proliferation [5-8]. Several GRPR agonists have been radiolabeled and tested preclinically [9, 10] and clinically [11, 12]. However, recent studies have indicated that GRPR antagonists show superior tumor uptake and image contrast, when compared to GRPR agonists [13, 14]. Furthermore, GRPR antagonists allow for a safer clinical use since no acute adverse effects (e.g., gastrointestinal) are expected.

In the past years, there have been several preclinical and clinical studies in prostate cancer targeting the GRPR [12, 15-18]. In contrast, there are only few studies focusing on GRPR imaging of BC. In a recent preclinical study Dalm et al. successfully imaged BC in mouse xenografts with small animal single-photon emission computed tomography/computed tomography (SPECT/CT) using a GRPR antagonist [4]. Prignon et al. visualized BC xenografts in mice using a  $^{68}\text{Ga}$ -labeled GRPR positron emission tomography (PET) tracer and found a potential superiority when compared to [ $^{18}\text{F}$ ]fluorodeoxyglucose (FDG)-PET [19]. However, only a few preliminary clinical studies on GRPR imaging in BC have been performed so far [20-22]. These consistently showed an increased GRPR expression in primary tumors and metastatic lymph nodes using  $^{99\text{m}}\text{Tc}$ -labeled and  $^{111}\text{In}$ -labeled GRPR agonists. These studies all share the same limitations of planar scintigraphy and SPECT-based imaging, which results in a low spatial resolution and sensitivity. Thus, the use of a GRPR ligand labeled with a positron emitter and state-of-the-art PET/CT is expected to provide a relevant diagnostic superiority compared to these early clinical approaches.

Our group has developed several highly promising GRPR antagonists, which have been successfully evaluated preclinically and clinically mainly focusing on prostate carcinoma [15, 16, 18, 23]. One of those ligands, the GRPR antagonist RM2, was

recently shown to be safe for use in humans [24]. In a consecutive study,  $^{68}\text{Ga}$ -RM2-PET/CT showed a good diagnostic accuracy for the diagnosis of primary prostate carcinoma [25]. On BC, no studies using this tracer have been reported to date.

The different molecular subtypes of BC include luminal A, luminal B, luminal B-like, Her2-neu positive and triple negative subtypes. While the luminal subtypes show high estrogen receptor (ER) expression and represent the most common subtypes with an excellent prognosis, the ER-low or ER-negative subtypes have higher recurrence rates and poorer prognosis [26]. Therefore, novel molecular diagnostic biomarkers may be helpful to optimize subtype-specific treatment in BC. Moreover, *in vitro* studies suggest a positive correlation between ER and GRPR expression [4, 27]. Thus, GRPR-PET/CT imaging may also provide information about ER receptor status of BC.

The aim of the present analysis was to evaluate the feasibility and possible value of GRPR-PET/CT in BC in a clinical setting and to determine if GRPR expression in BC is associated with typical prognostic parameters such as ER, progesterone receptor (PR) and HER2-neu expression, MIB-1 proliferation index and patient age.

## Material & Methods

### Patients

Fifteen female patients with newly diagnosed primary unilateral or bilateral BC in neoadjuvant and adjuvant treatment situation underwent  $^{68}\text{Ga}$ -RM2-PET/CT for staging purposes between July 2014 and February 2015 on compassionate-use basis. We intentionally only included patients with suspected locally advanced breast cancer as these patients presumably profit most from an extended staging. Furthermore, only patients were recruited that did not undergo any preceding local or systemic therapies that might interfere with GRPR binding. All patients gave written informed consent and the present data analysis was approved by the institutional ethical review board (496/14). The patient age (mean  $\pm$  standard deviation) was  $54.5 \pm 12.5$  years (range 33 - 75 years).

### Breast Core Biopsy

BC diagnosis was confirmed by core needle biopsy prior to  $^{68}\text{Ga}$ -RM2-PET/CT. In the case of clinically suspicious axillary lymph nodes an evaluation by core needle biopsy of lymph nodes was also performed. Time span between biopsy and  $^{68}\text{Ga}$ -RM2-PET/CT was  $14.9 \pm 8.1$  days (range 7 - 37 days).

In addition, suspicious findings on PET/CT

were re-assessed clinically by certified BC specialists; possibly affected axillary lymph nodes were verified by core needle biopsy, whereas internal mammary lymph nodes are not routinely assessed by ultrasound and biopsy at our institution.

### Immunohistochemistry

Tissue obtained by breast core biopsy was analyzed for ER and PR status, HER2/neu expression and MIB-1 proliferation index. Therefore, five serial tissue slices of 2  $\mu\text{m}$  thickness were prepared for immunohistochemistry (IHC) using a Leica RM2255 Microtome and stained afterwards for ER, PR, HER2/neu and MIB-1. Ready-to-use antibodies for ER (IR657, Clone 1D5), PR (IR068, Clone 636) and HER2/neu (A0485) were used for antigen detection. All slides were stained with Dako Real® Detection System (Dako K5001) according to the instructions of the manufacturer. Omission of primary antibody served as the negative control. For ER, PR and MIB-1, nuclear staining of non-tumoral mammary glands was used as internal positive control. For HER2/neu external controls form part of every run. A nuclear reactivity of ER and PR in > 1 % of the tumor cells was rated as a positive reaction. HER2/neu overexpression (HER 3+) was defined as an intense and complete membrane staining in more than 10 % of the tumor cells.

### Tracer synthesis

The RM2 precursor was provided by Piramal Imaging (Berlin, Germany). Radiolabelling of RM2 with  $^{68}\text{GaCl}_3$  was accomplished using a fully automated synthesis module (Pharmtracer, Eckert & Ziegler, Berlin, Germany). The automated preparation was done according to Good Manufacturing Practice under sterile conditions. Briefly, the  $^{68}\text{Ge}/^{68}\text{Ga}$  generator (IGG 100, Eckert & Ziegler) was eluted with 0.1 M HCl. Chemical purification and concentration of the generator eluate was carried out using a cation exchange resin (Strata x-c, Phenomenex).  $^{68}\text{Ga}$  (III) was eluted from the cartridge into the reaction vial using a 97.6 % acetone/0.02 N HCl solution. The reaction vial contained 60  $\mu\text{g}$  RM2 in 2 mL sodium acetate buffer (0.2 M, pH 4.0) and 200  $\mu\text{L}$  ethanol. Labelling was accomplished by heating the reaction mixture at 95°C for 10 min. For further purification, the solution was passed over a  $\text{C}_{18}$  light cartridge (Waters, USA), washed with 3 mL saline and eluted with 1 mL 50 % ethanol. The final product was constituted by addition of 7 mL saline and sterilized by filtration using Millex 0.22  $\mu\text{m}$  filter (Millipore, USA). Quality control was performed using an Agilent 1260 HPLC system with a Gina radioactivity detector (Raytest, Germany) in combination with a

ACE 3  $\text{C}_{18}$  (150 x 4.6 mm) column. The solvent system was A  $\text{H}_2\text{O}$  (0.1 % TFA) and B acetonitrile (0.1 % TFA). The gradient was 0 – 8 min 28 % B, 8 – 9 min 60 % B, 9 – 14 min 60 % B, 14 – 15 min 28 % B at a flow rate of 0.6 mL/min. The decay-corrected yield was > 90 % and the radiochemical purity of the final product was > 98 %. The product was sterile and pyrogen-free (< 0.5 EU/mL).

### $^{68}\text{Ga}$ -RM2-PET/CT

All patients received an intravenous injection of 118 – 213 MBq (3.19 – 5.76 mCi)  $^{68}\text{Ga}$ -RM2 (peptide dose 26 – 56  $\mu\text{g}$ ). Whole-body PET/CT scans were performed 1 h p.i. (2 min per bed position, contrast-enhanced diagnostic CT – 120 keV, 100 – 250 mAs, dose modulation, FOV 600  $\text{mm}^2$ , 512 x 512 matrix, slice thickness 2 mm) from the base of the skull to the proximal femur (64-slice GEMINI TF PET/CT, Philips Healthcare, Cleveland, USA). PET data were fully corrected for attenuation, scatter, decay and randoms and expressed as standardized uptake values (SUV; i.e., local radioactivity concentration normalized to injected dose per body weight).

### PET/CT analysis

PET images were analyzed by two experienced nuclear medicine physicians in consensus. PET-positivity was defined as focal tracer uptake of the primary tumor beyond local background in correlation with CT. Volume-of-interest (VOI) analysis was performed using PMOD (Ver. 3.205, PMOD Technologies, Zürich, Switzerland). The primary tumor was delineated under CT guidance on all transaxial slices and maximum SUV ( $\text{SUV}_{\text{MAX}}$ ) was calculated. Circular regions of interest (ROI) were placed on normal breast tissue (NBT) (diameter 30 mm), liver (diameter 40 mm), pancreas (diameter 20 mm), muscle (diameter 30 mm) and adipose tissue (diameter 30 mm) and mean SUV ( $\text{SUV}_{\text{MEAN}}$ ) as well as  $\text{SUV}_{\text{MAX}}$  were extracted. Lymph node sizes were assessed on contrast-enhanced diagnostic CT (CT portion of the PET/CT) measuring the long- and short-axis diameters on transaxial slices (voxel size 1.17 x 1.17 x 2  $\text{mm}^3$ ).

### Statistical Analysis

Analyses were performed using JMP (Ver. 11; SAS Institute, Cary, USA). PET positivity and SUV values were correlated with ER, PR, HER2/neu status and MIB-1 proliferation index in univariate analysis (Fisher's exact test for nominal and Spearman's rho ( $\rho$ ) for ordinal/continuous data). In addition, a multivariate analysis was performed with ER and PR expression, MIB-1 proliferation index (each expressed

as percent) and HER2/neu status (binary categorical) as independent variables to predict the observed  $SUV_{MAX}$  value (dependent variable).

## Results

Three patients presented with bilateral tumors. Histological tumor types were 14 no special type (NST; formerly classified as invasive ductal carcinoma), 3 invasive lobular carcinoma (ILC) and 1 mucinous carcinoma (MC). Patient characteristics and imaging findings, including lymph node (LN) findings are summarized in Table 1. No adverse effects were observed during or following the administration of  $^{68}\text{Ga}$ -RM2.

NBT showed an intra- and interindividually variable, moderately strong  $^{68}\text{Ga}$ -RM2 binding with a  $SUV_{MEAN}$   $1.1 \pm 0.5$  and an  $SUV_{MAX}$   $2.3 \pm 1.0$ . Physiological biodistribution demonstrated little  $^{68}\text{Ga}$ -RM2 uptake in fat ( $SUV_{MEAN}$   $0.2 \pm 0.04$ ) and muscle ( $SUV_{MEAN}$   $0.4 \pm 0.10$ ), moderate uptake in liver ( $SUV_{MEAN}$   $1.1 \pm 0.3$ ) and intense uptake in pancreas ( $SUV_{MEAN}$   $40.8 \pm 9.8$ ), which corresponds to earlier studies [11, 16]. Furthermore a weak negative association between  $^{68}\text{Ga}$ -RM2 uptake of NBT and patient age was observed, which however did not reach a level of statistical significance on univariate analysis (Spearman's  $\rho = -0.36$ ;  $p = 0.14$ ).

13/18 tumors were clearly visualized by increased  $^{68}\text{Ga}$ -RM2 uptake compared to NBT and thus rated as PET-positive (Figure 1). Mean  $SUV_{MAX}$  of PET-positive tumors was  $11.2 \pm 5.8$  (range 3.9 – 22.5). 5/18 tumors could not be differentiated from NBT and thus were defined as PET-negative. Mean

$SUV_{MAX}$  of PET-negative tumors was  $2.4 \pm 0.9$  (range 1.4 – 3.5). However, in these cases, metastatic manifestations (i.e., metastatic axillary lymph nodes) could still be identified clearly in regions with low physiological tracer uptake (Figure 2).  $SUV_{MAX}$  of the primary tumor did not correlate with patient age ( $p = 0.71$ ).

All tumors rated PET-positive were also positive for ER and PR expression, in contrast to only 1/5 tumors visually rated PET-negative (Patient No. 13;  $SUV_{MAX}$  3.0). The single PET-negative, ER-positive tumor was a mucinous carcinoma with an immunohistochemical ER expression of 30 % and a PR expression of 40 %. Mean  $SUV_{MAX}$  of ER-positive tumors was  $10.6 \pm 6.0$  compared to  $2.3 \pm 1.0$  in ER-negative tumors ( $p = 0.016$ ). NST and ILC did show comparable  $SUV_{MAX}$  values (NST  $9.2 \pm 6.9$ , ILC  $8.9 \pm 4.1$ ;  $p = 0.92$ ). All ER-positive tumors were also positive for PR status. PET positivity was significantly associated with ER status (Fisher's exact test,  $p = 0.0016$ ) and PR status ( $p = 0.0016$ ), but not with HER2/neu status ( $p = 0.07$ ). For quantitative PET measures (i.e.,  $SUV_{MAX}$ ) and relative biomarker expressions (i.e., ER, PR, MIB-1 in percent), significant correlations were found for ER (Spearman's  $\rho = 0.70$ ,  $p = 0.0013$ ) and PR ( $\rho = 0.50$ ;  $p = 0.038$ ), but not for MIB-1 ( $\rho = -0.13$ ,  $p = 0.61$ ). As may be expected, ER and PR expression was correlated ( $\rho = 0.72$ ,  $p = 0.0007$ ). In a multivariate analysis including ER, PR, HER2/neu and MIB-1 as predictor variables, only ER expression predicted  $^{68}\text{Ga}$ -RM2 uptake (model:  $r^2 = 0.55$ ,  $p = 0.025$ ; parameter estimates: ER  $p = 0.0075$ , all other parameters  $p > 0.15$ ) (Figure 3).

**Table 1.** Patient biopsy characteristics and imaging findings.

Patient No	Type/Side	Immunohistochemistry				Image findings		
		ER	PR	HER2/neu	MIB-1 Index	PET Rating	LN No. and location (CT)	LN size /mm (CT)
1	NST / bilateral	+	+	-	40%	pos	left: > 5 ax / 3 IMLN	3x3 – 11x7
2	NST / left	+	+	-	40%	pos	> 5 ax / 4 IMLN	15x10 – 11x6
3	ILC / right	+	+	-	27%	pos	1 ax	10x9
4	NST / right	-	-	-	90%	neg	2 IMLN	5x3 – 24x20
5	NST / right	+	+	-	8%	pos	1 ax	14x6
6	ILC / right	+	+	-	30%	pos	/	/
7	NST / bilateral	right: + left: -	right: + left: -	right: - left: +	right: 18 % left: 20 %	right: pos left: neg	/	/
8	NST / left	-	-	-	80%	neg	5 IMLN	7x7 – 11x14
9	NST / bilateral	+	+	-	right: 18 % left: 15 %	pos	right: 2 ax / 1 IMLN	3x4 – 11x5
10	ILC / left	+	+	-	15%	pos	/	/
11	NST / right	+	+	-	16%	pos	/	/
12	NST / right	-	-	-	60%	neg	> 5 ax / 1 IMLN / 1 scl / 1 spc	6x6 – 9x9
13	MC / right	+	+	+	20%	neg	> 5 ax	9x8 – 42x24
14	NST / right	+	+	-	23%	pos	> 5 ax / 5 IMLN / 2 med / 1 hil	3x4 – 22x15
15	NST / left	+	+	-	38%	pos	> 5 ax / 4 IMLN / 9 spc / 1 cl	3x3 – 14x19

Abbreviations: pos, positive; neg, negative; LN, lymph node; ax, axillary; IMLN, internal mammary lymph node; med, mediastinal; hil, hilar; spc, subpectoral; scl, supraclavicular; cl, contralateral axillary; for additional abbreviations see text.

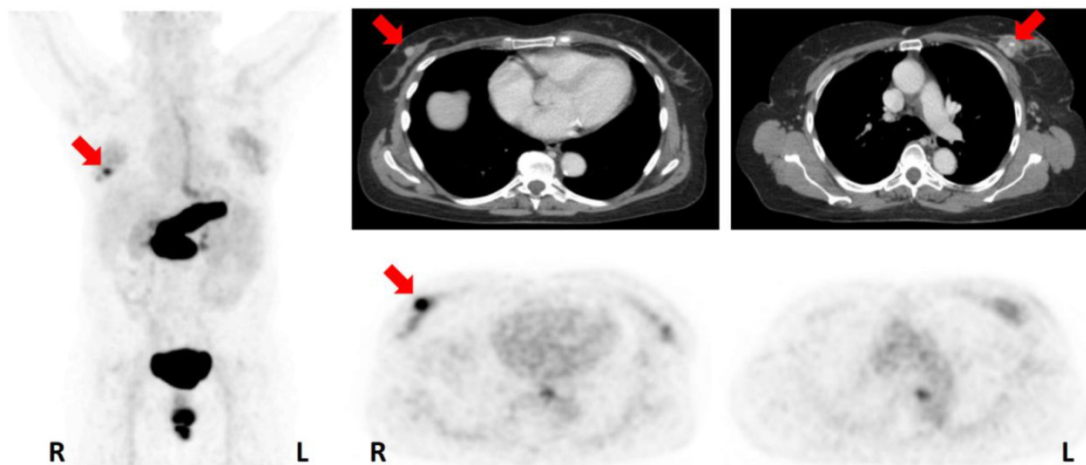


**Figure 1.** 74-year-old patient (No. 7) with a bilateral NST with an ER/PR-positive tumor on the right side (PET-positive;  $SUV_{MAX}$  8.32) and an ER/PR-negative tumor on the left side (PET-negative;  $SUV_{MAX}$  2.68). Maximum intensity projection (left); CT (upper row);  $^{68}Ga$ -RM2-PET (lower row); primary tumors indicated by red arrows. Note the physiological uptake in the pancreas, esophagus and rectum. For abbreviations see text.

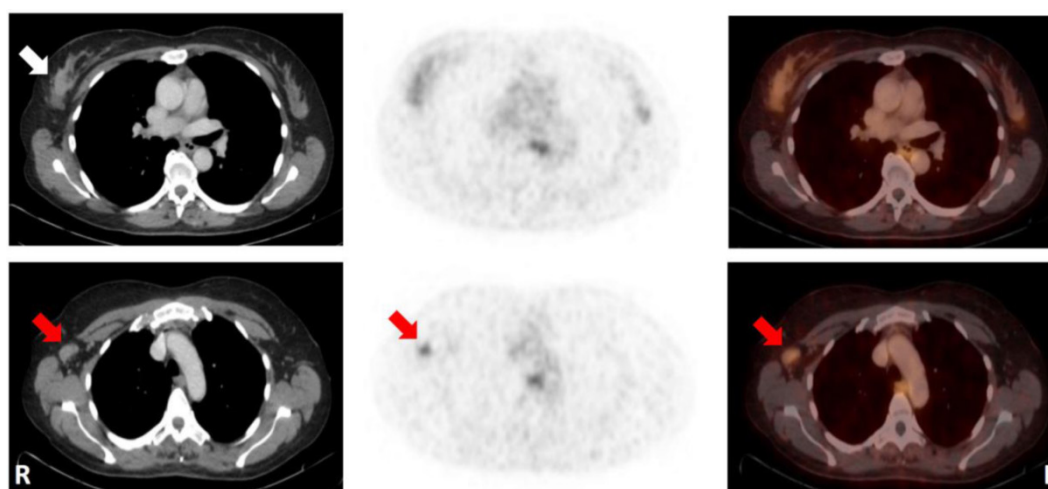


**Figure 2.** 50-year-old patient (No. 13) with a mucinous carcinoma of the right breast with low ER/PR-expression. Note that the primary tumor could not be distinguished from normal breast tissue, while an ipsilateral axillary lymph node metastasis (histologically proven;  $SUV_{MAX}$  2.9) was identified by increased  $^{68}Ga$ -RM2-uptake relative to the surrounding tissue. CT (left);  $^{68}Ga$ -RM2-PET (middle); fusion images (right); primary tumor indicated by white arrow; lymph node metastasis indicated by red arrows. For abbreviations see text.

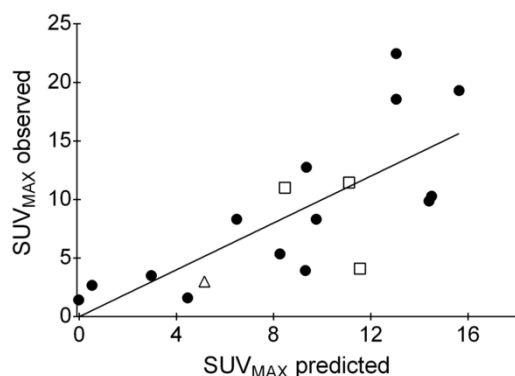


**Figure 3.** Result of the multivariate analysis. Observed  $SUV_{MAX}$  values (y-axis) were plotted over predicted  $SUV_{MAX}$  values (x-axis; included predictor variables: ER and PR expression, MIB-1 proliferation index (each expressed as percent) and HER2/neu status (binary categorial)). ER expression is the only statistically significant predictor of  $SUV_{MAX}$ . Symbols: filled circles, no special type; open squares, invasive lobular carcinomas; open triangle, mucinous carcinoma. For abbreviations see text.

Given the paucity of data on the clinical diagnostic value of GRPR-PET, suspicious findings of possible therapeutic relevance were only accepted as true findings if confirmed by CT or biopsy.  $^{68}Ga$ -RM2-PET/CT revealed a possible upstaging compared to conventional clinical staging (i.e. breast, axillary and abdominal ultrasound, chest x-ray and bone scan; conventional clinical staging does not include ultrasound of internal mammary lymph nodes or FDG-PET/CT) in 7/15 (47 %) of the examined BC patients including 6 to stage III and 1 to stage IV (Table 2). In 8 patients internal mammary lymph nodes (IMLN), strongly positive on  $^{68}Ga$ -RM2-PET and rated as suspicious for malignancy by CT (size 3 to 19 mm), were detected, in line with an possible upstaging to stage IIIA and IIIC in 6 patients (Figure 4A). Upstaging to stage IV

occurred in one patient due to the detection of a contralateral axillary lymph node metastasis verified by biopsy (Figure 4B).

In one patient several bone metastases were detected on bone scan and CT. All lesions also showed high  $^{68}\text{Ga}$ -RM2 uptake. However, several additional lesions were depicted by increased focal  $^{68}\text{Ga}$ -RM2 uptake in PET, but not detected by CT or bone scan (Figure 4C).

**Table 2.** Primary clinical and  $^{68}\text{Ga}$ -RM2-PET/CT stages <sup>1</sup>.

Primary clinical stage	Total cases	$^{68}\text{Ga}$ -RM2-PET/CT stage							Upstaged cases n (%)
		IA	IIA	IIB	IIIA	IIIB	IIIC	IV	
IA	2	2							0 (0)
IIA	5		2		2*		1*		3 (60)
IIB	3			1*			2		2 (66)
IIIA	3				1		1	1	2 (67)
IIIB	1					1			0 (0)
IIIC	-								-
IV	1							1	0 (0)
Total	15								7 (47)

<sup>1</sup> According to the 7<sup>th</sup> Ed. of the AJCC Cancer Staging Manual [49].

\*Patient with a bilateral tumors.

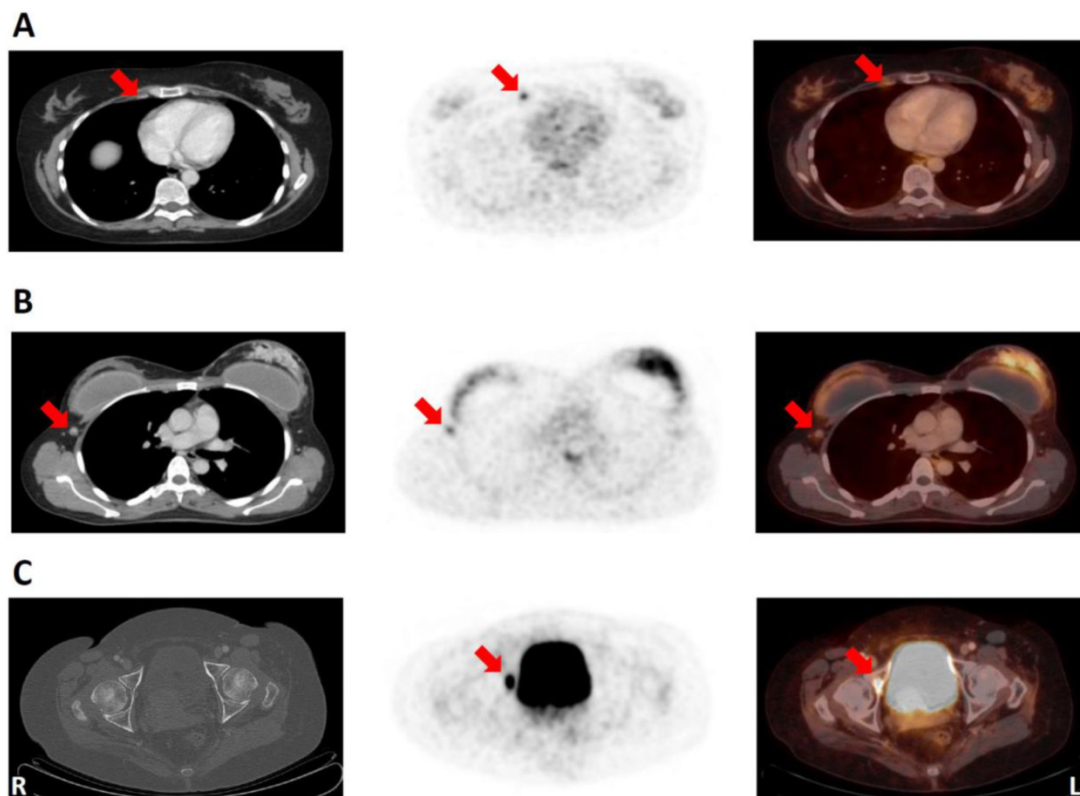


**Figure 4.** **A:** 50-year-old patient (No. 1) with bilateral ER/PR-positive NST. Note the detection of a very small (3x3 mm) internal mammary lymph node (IMLN) with intensive  $^{68}\text{Ga}$ -RM2-uptake ( $\text{SUV}_{\text{MAX}}$  3.8). CT (left);  $^{68}\text{Ga}$ -RM2-PET (middle); fusion image (right); suspicious IMLN (lateral to internal mammary vessels) indicated by red arrows. **B:** 43-year-old patient (No. 15) with a ER/PR-positive NST of the left breast. Note the contralateral axillary lymph node metastasis with increased GRPR expression (verified by biopsy;  $\text{SUV}_{\text{MAX}}$  2.6). CT (left);  $^{68}\text{Ga}$ -RM2-PET (middle); fusion image (right); contralateral lymph node metastasis indicated by red arrows. **C:** 80-year-old patient (No. 14) with an ER/PR-positive NST of the right breast. CT did not show any noticeable bone alteration, while  $^{68}\text{Ga}$ -RM2-PET depicted intense focal gastrin-releasing peptide receptor expression in the right acetabulum (among other locations) highly suspicious of a bone metastasis ( $\text{SUV}_{\text{MAX}}$  14.3). CT (left);  $^{68}\text{Ga}$ -RM2-PET (middle); fusion image (right). Suspicious bone lesion indicated by red arrows. For abbreviations see text.

## Discussion

The present study demonstrates that  $^{68}\text{Ga}$ -RM2-PET/CT is capable of *in vivo* visualizing GRPR expression with high contrast in the majority of the examined BC patients (73 %; 11/15). Our data are in accordance with the *in vitro* results obtained by Reubi et al. [2, 3]. Apart from NST, we were also able to clearly visualize all ILC, which may be missed by conventional FDG-PET/CT due to often limited FDG

avidity [28]. While univariate analyses revealed a strong association between GRPR binding and ER as well as PR status, a multivariate regression analysis identified ER as the primary predictor of  $^{68}\text{Ga}$ -RM2 uptake. Therefore,  $^{68}\text{Ga}$ -RM2-PET/CT may provide a promising imaging modality with high image quality in patients with ER-positive tumors, representing the majority of BC cases (81 % in a recent study examining a diverse patient population [29]).

The positive correlation between GRPR binding and ER expression, which we found in our in vivo study, is in line with previous in vitro studies: Halmos et al. showed a significant association between high-affinity binding of the GRPR agonist  $^{125}\text{I}$ -Tyr<sup>4</sup>-bombesin on isolated cell membranes and estrogen receptor expression in BC biopsy specimens ( $r = 0.671, p < 0.005$ ) [27]. Similarly, Dalm et al. found a significant positive correlation ( $p = 0.026$ ) between the extent of GRPR expression detected by autoradiography with the GRPR agonist  $^{111}\text{In}$ -AMBA (5-step score) and ER status in BC tissue specimens [4]. This was confirmed by a subsequent study by the same group, demonstrating a significant positive association ( $p < 0.001$ ) between GRPR messenger RNA (mRNA) and ER positivity in BC [30]. Interestingly, GRPR mRNA levels correlated significantly with prolonged progression-free survival in metastatic ER-positive BC patients undergoing tamoxifen treatment [30]. These findings underline the potential clinical relevance of GRPR imaging in BC patients.

To the best of our knowledge the mechanism for the correlation between ER expression and the expression of GRPR and other G protein couple receptors are not well understood are not well understood and needs further studies [31] [32].

Albeit our findings warrant verification by larger patient series, it is tempting to speculate about potential clinical indications of GRPR PET in BC patients. For instance, in clinical practice the hormone receptor status is usually already known at time of the initial diagnosis by biopsy. This information could be used for a personalized selection of the staging strategy that may include GRPR PET/CT in ER-positive tumors. Furthermore, GRPR PET/CT may allow investigators to assess ER expression levels non-invasively in whole-body imaging studies. This could provide unique opportunities to study the heterogeneity of ER expression. Of note, tumor heterogeneity between the primary tumor and synchronous metastases seems to be less than in the situation of metachronous metastases [33]. On one hand, this supports the use of GRPR PET for initial staging of known ER-positive primary tumors. On the other, if the correlation between GRPR binding and ER expression holds true also in the course of the disease and its various treatments, GRPR PET may also be helpful to uncover a possibly increasing heterogeneity of the ER status over time (e.g., loss of ER expression or occurrence of new ER-negative manifestations). This may be of important therapeutic and prognostic implications (e.g., for endocrine therapy or targeted radionuclide therapy).

ER status of BC can be images with the ER ligand  $16\alpha$ -[ $^{18}\text{F}$ ]-fluoro- $17\beta$ -oestradiol (FES) PET imaging of

in vivo ER expression by employing ER-specific ligands. In a meta-analysis of 4 studies, van Kruchten et al. calculated an overall sensitivity of FES-PET of 84 % for the detection of ER-positive BC [34]. The correlation coefficients for the relationship of  $^{18}\text{F}$ -FES uptake and ER expression ranged from 0.56 – 0.96 [34-36]. In our study,  $^{68}\text{Ga}$ -RM2 binding to GRPR correlated well with ER expression (Spearman's  $\rho = 0.70, p = 0.0013$ ), which is in the same range as for  $^{18}\text{F}$ -FES. Possible advantages of  $^{68}\text{Ga}$ -RM2-PET/CT compared to  $^{18}\text{F}$ -FES-PET/CT include a more favorable biodistribution for tumor staging due to much lower liver and intestinal radiotracer uptake. In addition,  $^{68}\text{Ga}$ -RM2 binding to GRPR is less likely to be affected by endogenous estrogen levels (e.g., differences between pre- and postmenopausal patients), sex hormone-binding globulin serum levels and anti-estrogen treatment. However, it remains to be seen if and to what extent these factors affect GRPR expression and thus  $^{68}\text{Ga}$ -RM2 uptake as a prerequisite for the possible use of GRPR PET in pre-treated patients and for treatment monitoring.

FDG-PET/CT is a valuable diagnostic tool for the detection of distant metastases [37, 38]. Its role for evaluation of locoregional lymph node status on the other hand is controversial. According to a recent review the sensitivity of FDG-PET/CT for the detection of axillary lymph nodes ranges between 24 and 82 % [39]. There are some limitations of FDG-PET imaging that may lead to reduced diagnostic accuracy. Inflammatory reactions may mimic tumor infestation and thus lead to false positive results [40]. Small tumor manifestations might be missed by PET due to the limited spatial resolution and contrast compared to background. In the present study  $^{68}\text{Ga}$ -RM2-PET/CT allowed us to visualize affected lymph nodes less than 5 mm in maximum diameter due the very low radiotracer uptake in muscles and fat tissue. The low background also allows for the detection of lymph node metastases of primary tumors with little GRPR expression.

In our preliminary analysis, we found a potential clinical upstaging of 47 % of the examined patients (7/15) after  $^{68}\text{Ga}$ -RM2-PET/CT due to the detection of suspicious lymph nodes.  $^{68}\text{Ga}$ -RM2-PET/CT showed a high detection rate for suspicious IMLN (53 %; 8/15), leading to potential upstaging of 40 % of the patients (6/15). A recently published study using FDG-PET/CT found suspicious IMLN in 62/216 patients (29 %) [41]. We hypothesize that the high detection rate observed in our study is due to the intense uptake of  $^{68}\text{Ga}$ -RM2-PET/CT by ER-positive BC and the very low physiologic uptake of  $^{68}\text{Ga}$ -RM2-PET/CT in fat and muscle tissue. However, this hypothesis needs to be tested in studies

performing an intra-individual comparison of FDG-PET/CT and  $^{68}\text{Ga}$ -RM2-PET/CT.

The clinical relevance of suspicious internal mammary lymph nodes on patient outcome has been discussed controversially in literature. Hennequin et al. for example show no apparent survival benefit when performing external beam irradiation of IMLNs [42], while Chang et al. suggest a significant longer disease-free survival [43]. Regarding the detection of distant bone metastases,  $^{68}\text{Ga}$ -RM2-PET not only identified metastases also detected by CT and bone scan, but also showed suspicious bone lesions solely positive on  $^{68}\text{Ga}$ -RM2-PET. Interestingly an earlier study using a GRPR agonist and scintigraphic imaging in tamoxifen-resistant BC (n = 5) could not identify known bone metastases [21]. While these results are highly promising for imaging ER-positive tumors, further evaluation in larger patient series and systematic histologic validation are obviously needed.

In addition to diagnosis, GRPR targeting could provide a new therapeutic approach via peptide receptor radionuclide therapy (PRRT) in patients with GRPR-positive BC, as already practiced for neuroendocrine tumors, where somatostatin receptor-targeting PRRT has become a very important asset [44-47]. GRPR antagonists, such as RM2, labeled with a therapeutic radioisotope (e.g., lutetium-177) could be used to treat BC patients while using Ga-68 labeled RM2 as a diagnostic companion in a theranostic treatment concept. We observed high physiological uptake in pancreatic tissue, which according to GRPR blockade studies in mice is most likely due to specific GRPR binding [48]. Given the faster washout of GRPR antagonists from the pancreas than from prostate cancer tissue observed in previous preclinical [15, 18] and clinical [16] studies, the radiation dose to the pancreas is expected to be significantly lower than the radiation dose to tumor manifestations. Dosimetric studies employing long-lived nuclides (e.g., Lu-177) and dynamic data acquisition are needed to explore in how far pancreatic uptake may limit the therapeutic application of GRPR antagonists compared to other small molecules (e.g., ER-targeting agents). However, in a murine prostate cancer model long-term tumor regression could be achieved by treatment with  $^{177}\text{Lu}$ -DOTA-RM2 without evidence for damage to the pancreas [15].

Limitations of our study are the relatively low number of patients, which renders our multivariate analysis preliminary. Albeit our preliminary results suggest a diagnostic value of  $^{68}\text{Ga}$ -RM2-PET/CT in ER-positive BC (i.e., sensitivity of 93% for ER-positive tumors, upstaging in 47% of patients), this needs to be verified by future studies. For calculation of

diagnostic parameters like sensitivity, specificity and accuracy, studies need to include larger patient cohorts with various suspicious breast lesions and to pursue a comprehensive pathological verification of detected lesions (i.e., with and without increased  $^{68}\text{Ga}$ -RM2 uptake, breast and metastatic lesions). The present patient sample comprises only patients with known BC, while possible false-positive lesions (e.g., fibroadenoma [22]) were not observed. Furthermore, not all suspicious lymph nodes (in particular IMLN) detected by  $^{68}\text{Ga}$ -RM2-PET/CT were histologically confirmed. Thus, it has to be emphasized that aforementioned results concerning the potential upstaging of patients need further validation. Finally, we did not pursue a detailed head-to-head comparison of FDG-PET with  $^{68}\text{Ga}$ -RM2-PET/CT. Such studies are needed to define possible benefits of one method over the other for a given clinical condition (e.g., tumor types NST vs. ILM, ER status positive vs. negative) and method-specific drawbacks (e.g., physiological GRPR expression in breast tissue or increased FDG uptake in inflammatory lymph nodes).

## Conclusion

Our study demonstrates that  $^{68}\text{Ga}$ -RM2-PET/CT is a promising imaging method in BC patients, especially for ER-positive tumors. *In vivo* GRPR binding assessed by  $^{68}\text{Ga}$ -RM2-PET/CT correlated with ER expression in primary tumors of untreated BC patients.

## Acknowledgements

We thank Piramal Imaging for providing the precursor to support this study.

## Competing Interests

Philipp T Meyer and Wolfgang A Weber receive financial support from Piramal Imaging for an ongoing research project (outside the submitted work). Helmut R Maecke is a co-inventor of a patent for bombesin receptor antagonists.

## References

1. Reubi JC, Fleischmann A, Waser B, Rehm R. Concomitant vascular GRP-receptor and VEGF-receptor expression in human tumors: molecular basis for dual targeting of tumoral vasculature. *Peptides*. 2011; 32: 1457-62.
2. Reubi JC, Wenger S, Schmuckli-Maurer J, Schaer JC, Gugger M. Bombesin receptor subtypes in human cancers: detection with the universal radioligand (125)I-[D-TYR(6), beta-ALA(11), PHE(13), NLE(14)] bombesin(6-14). *Clinical cancer research : an official journal of the American Association for Cancer Research*. 2002; 8: 1139-46.
3. Reubi C, Gugger M, Waser B. Co-expressed peptide receptors in breast cancer as a molecular basis for in vivo multireceptor tumour targeting. *European journal of nuclear medicine and molecular imaging*. 2002; 29: 855-62.
4. Dalm SU, Martens JW, Sieuwerts AM, van Deurzen CH, Koelwijns SJ, de Blois E, et al. In vitro and in vivo application of radiolabeled gastrin-releasing peptide receptor ligands in breast cancer. *Journal of nuclear medicine : official publication, Society of Nuclear Medicine*. 2015; 56: 752-7.

5. Yano T, Pinski J, Groot K, Schally AV. Stimulation by bombesin and inhibition by bombesin/gastrin-releasing peptide antagonist RC-3095 of growth of human breast cancer cell lines. *Cancer research*. 1992; 52: 4545-7.
6. Nelson J, Donnelly M, Walker B, Gray J, Shaw C, Murphy RF. Bombesin stimulates proliferation of human breast cancer cells in culture. *British journal of cancer*. 1991; 63: 933-6.
7. Lango MN, Dyer KF, Lui VW, Gooding WE, Gubish C, Siegfried JM, et al. Gastrin-releasing peptide receptor-mediated autocrine growth in squamous cell carcinoma of the head and neck. *Journal of the National Cancer Institute*. 2002; 94: 375-83.
8. Moody TW, Leyton J, Garcia-Marin L, Jensen RT. Nonpeptide gastrin releasing peptide receptor antagonists inhibit the proliferation of lung cancer cells. *European journal of pharmacology*. 2003; 474: 21-9.
9. Chen X, Park R, Hou Y, Tohme M, Shahinian AH, Bading JR, et al. microPET and autoradiographic imaging of GRP receptor expression with <sup>64</sup>Cu-DOTA-[Lys<sup>3</sup>]bombesin in human prostate adenocarcinoma xenografts. *Journal of nuclear medicine : official publication, Society of Nuclear Medicine*. 2004; 45: 1390-7.
10. Lantry LE, Cappelletti E, Maddalena ME, Fox JS, Feng W, Chen J, et al. <sup>177</sup>Lu-AMBA: Synthesis and characterization of a selective <sup>177</sup>Lu-labeled GRP-R agonist for systemic radiotherapy of prostate cancer. *Journal of nuclear medicine : official publication, Society of Nuclear Medicine*. 2006; 47: 1144-52.
11. Van de Wiele C, Dumont F, Vanden Broecke R, Oosterlinck W, Cocquyt V, Serreyn R, et al. Technetium-99m RP527, a GRP analogue for visualisation of GRP receptor-expressing malignancies: a feasibility study. *European journal of nuclear medicine*. 2000; 27: 1694-9.
12. Bodei L, Ferrari M, Nunn A. <sup>177</sup>Lu-AMBA Bombesin analogue in hormone refractory prostate cancer patients: a phase I escalation study with single-cycle administrations [abstract]. *European journal of nuclear medicine and molecular imaging*. 2007; (Suppl 2): S221.
13. Cescato R, Maina T, Nock B, Nikolopoulou A, Charalambidis D, Piccard V, et al. Bombesin receptor antagonists may be preferable to agonists for tumor targeting. *Journal of nuclear medicine : official publication, Society of Nuclear Medicine*. 2008; 49: 318-26.
14. Mansi R, Wang X, Forrer F, Kneifel S, Tamma ML, Waser B, et al. Evaluation of a <sup>14,7,10</sup>-tetraazacyclododecane-1,4,7,10-tetraacetic acid-conjugated bombesin-based radioantagonist for the labeling with single-photon emission computed tomography, positron emission tomography, and therapeutic radionuclides. *Clinical cancer research : an official journal of the American Association for Cancer Research*. 2009; 15: 5240-9.
15. Dumont RA, Tamma M, Braun F, Borkowski S, Reubi JC, Maecke H, et al. Targeted radiotherapy of prostate cancer with a gastrin-releasing peptide receptor antagonist is effective as monotherapy and in combination with rapamycin. *Journal of nuclear medicine : official publication, Society of Nuclear Medicine*. 2013; 54: 762-9.
16. Wieser G, Mansi R, Grosu AL, Schultze-Seemann W, Dumont-Walter RA, Meyer PT, et al. Positron emission tomography (PET) imaging of prostate cancer with a gastrin releasing peptide receptor antagonist—from mice to men. *Theranostics*. 2014; 4: 412-9.
17. Liu Y, Hu X, Liu H, Bu L, Ma X, Cheng K, et al. A comparative study of radiolabeled bombesin analogs for the PET imaging of prostate cancer. *Journal of nuclear medicine : official publication, Society of Nuclear Medicine*. 2013; 54: 2132-8.
18. Mansi R, Abiraj K, Wang X, Tamma ML, Gourni E, Cescato R, et al. Evaluation of three different families of bombesin receptor radioantagonists for targeted imaging and therapy of gastrin releasing peptide receptor (GRP-R) positive tumors. *Journal of medicinal chemistry*. 2015; 58: 682-91.
19. Prignon A, Nataf V, Provost C, Cagnolini A, Montravers F, Gruaz-Guyon A, et al. <sup>68</sup>Ga-AMBA and <sup>18</sup>F-FDG for preclinical PET imaging of breast cancer: effect of tamoxifen treatment on tracer uptake by tumor. *Nuclear medicine and biology*. 2015; 42: 92-8.
20. Scopinaro F, Varvarigou AD, Ussof W, De Vincentis G, Sourlingas TG, Evangelatos GP, et al. Technetium labeled bombesin-like peptide: preliminary report on breast cancer uptake in patients. *Cancer biotherapy & radiopharmaceuticals*. 2002; 17: 327-35.
21. Van de Wiele C, Phonteyne P, Pauwels P, Goethals I, Van den Broecke R, Cocquyt V, et al. Gastrin-releasing peptide receptor imaging in human breast carcinoma versus immunohistochemistry. *Journal of nuclear medicine : official publication, Society of Nuclear Medicine*. 2008; 49: 260-4.
22. Shariati F, Aryana K, Fattahi A, Forghani MN, Azarian A, Zakavi SR, et al. Diagnostic value of <sup>99m</sup>Tc-bombesin scintigraphy for differentiation of malignant from benign breast lesions. *Nuclear medicine communications*. 2014; 35: 620-5.
23. Gourni E, Mansi R, Jamous M, Waser B, Smerling C, Burian A, et al. N-terminal modifications improve the receptor affinity and pharmacokinetics of radiolabeled peptidic gastrin-releasing peptide receptor antagonists: examples of <sup>68</sup>Ga- and <sup>64</sup>Cu-labeled peptides for PET imaging. *Journal of nuclear medicine : official publication, Society of Nuclear Medicine*. 2014; 55: 1719-25.
24. Roivainen A, Kahkonen E, Luoto P, Borkowski S, Hofmann B, Jambor I, et al. Plasma pharmacokinetics, whole-body distribution, metabolism, and radiation dosimetry of <sup>68</sup>Ga bombesin antagonist BAY 86-7548 in healthy men. *Journal of nuclear medicine : official publication, Society of Nuclear Medicine*. 2013; 54: 867-72.
25. Kahkonen E, Jambor I, Kempainen J, Lehtio K, Gronroos TJ, Kuisma A, et al. In vivo imaging of prostate cancer using <sup>68</sup>Ga-labeled bombesin analog BAY86-7548. *Clinical cancer research : an official journal of the American Association for Cancer Research*. 2013; 19: 5434-43.
26. Loi S, Haibe-Kains B, Desmedt C, Lallemand F, Tutt AM, Gillet C, et al. Definition of clinically distinct molecular subtypes in estrogen receptor-positive breast carcinomas through genomic grade. *J Clin Oncol*. 2007; 25: 1239-46.
27. Halmos G, Wittliff JL, Schally AV. Characterization of bombesin/gastrin-releasing peptide receptors in human breast cancer and their relationship to steroid receptor expression. *Cancer research*. 1995; 55: 280-7.
28. Hogan MP, Goldman DA, Dashevsky B, Riedl CC, Gonen M, Osborne JR, et al. Comparison of 18F-FDG PET/CT for Systemic Staging of Newly Diagnosed Invasive Lobular Carcinoma Versus Invasive Ductal Carcinoma. *Journal of nuclear medicine : official publication, Society of Nuclear Medicine*. 2015; 56: 1674-80.
29. Wan D, Villa D, Woods R, Yerushalmi R, Gelmon K. Breast Cancer Subtype Variation by Race and Ethnicity in a Diverse Population in British Columbia. *Clinical breast cancer*. 2015.
30. Dalm SU, Sieuwerts AM, Look MP, Melis M, van Deurzen CH, Foekens JA, et al. Clinical Relevance of Targeting the Gastrin-Releasing Peptide Receptor, Somatostatin Receptor 2, or Chemokine C-X-C Motif Receptor 4 in Breast Cancer for Imaging and Therapy. *Journal of nuclear medicine : official publication, Society of Nuclear Medicine*. 2015; 56: 1487-93.
31. Nagasaki S, Nakamura Y, Maekawa T, Akahira J, Miki Y, Suzuki T, et al. Immunohistochemical analysis of gastrin-releasing peptide receptor (GRPR) and possible regulation by estrogen receptor beta in human prostate carcinoma. *Neoplasia*. 2012; 59: 224-32.
32. Rivera JA, Alturaihi H, Kumar U. Differential regulation of somatostatin receptors 1 and 2 mRNA and protein expression by tamoxifen and estradiol in breast cancer cells. *Journal of carcinogenesis*. 2005; 4: 10.
33. Martelotto LG, Ng CK, Piscuoglio S, Weigelt B, Reis-Filho JS. Breast cancer intra-tumor heterogeneity. *Breast cancer research : BCR*. 2014; 16: 210.
34. Van Kruchten M, de Vries EG, Brown M, de Vries EF, Glaudemans AW, Dierckx RA, et al. PET imaging of oestrogen receptors in patients with breast cancer. *The Lancet Oncology*. 2013; 14: e465-75.
35. Peterson LM, Mankoff DA, Lawton T, Yagle K, Schubert EK, Stekhova S, et al. Quantitative imaging of estrogen receptor expression in breast cancer with PET and 18F-fluoroestradiol. *Journal of nuclear medicine : official publication, Society of Nuclear Medicine*. 2008; 49: 367-74.
36. Mintun MA, Welch MJ, Siegel BA, Mathias CJ, Brodack JW, McGuire AH, et al. Breast cancer: PET imaging of estrogen receptors. *Radiology*. 1988; 169: 45-8.
37. Groheux D, Hindie E, Delord M, Giacchetti S, Hamy AS, de Bazelaine C, et al. Prognostic impact of (18)FDG-PET-CT findings in clinical stage III and IIB breast cancer. *Journal of the National Cancer Institute*. 2012; 104: 1879-87.
38. Riedl CC, Slobod E, Jochelson M, Morrow M, Goldman DA, Gonen M, et al. Retrospective analysis of 18F-FDG PET/CT for staging asymptomatic breast cancer patients younger than 40 years. *Journal of nuclear medicine : official publication, Society of Nuclear Medicine*. 2014; 55: 1578-83.
39. Liu Y. Role of FDG PET-CT in evaluation of locoregional nodal disease for initial staging of breast cancer. *World journal of clinical oncology*. 2014; 5: 982-9.
40. Shreve PD, Anzai Y, Wahl RL. Pitfalls in oncologic diagnosis with FDG PET imaging: physiologic and benign variants. *Radiographics : a review publication of the Radiological Society of North America, Inc*. 1999; 19: 61-77; quiz 150-1.
41. Seo MJ, Lee JJ, Kim HO, Chae SY, Park SH, Ryu JS, et al. Detection of internal mammary lymph node metastasis with (18)F-fluorodeoxyglucose positron emission tomography/computed tomography in patients with stage III breast cancer. *European journal of nuclear medicine and molecular imaging*. 2014; 41: 438-45.
42. Hennequin C, Bossard N, Servagi-Vernat S, Maingon P, Dubois JB, Datchary J, et al. Ten-year survival results of a randomized trial of irradiation of internal mammary nodes after mastectomy. *International journal of radiation oncology, biology, physics*. 2013; 86: 860-6.
43. Chang JS, Park W, Kim YB, Lee JJ, Keum KC, Lee CG, et al. Long-term survival outcomes following internal mammary node irradiation in stage II-III breast cancer: results of a large retrospective study with 12-year follow-up. *International journal of radiation oncology, biology, physics*. 2013; 86: 867-72.
44. Imhof A, Brunner P, Marincek N, Briel M, Schindler C, Rasch H, et al. Response, survival, and long-term toxicity after therapy with the radiolabeled somatostatin analogue <sup>90</sup>Y-DOTA-TOC in metastasized neuroendocrine cancers. *J Clin Oncol*. 2011; 29: 2416-23.
45. Fani M, Maecke HR. Radiopharmaceutical development of radiolabelled peptides. *European journal of nuclear medicine and molecular imaging*. 2012; 39 (Suppl 1): S11-30.
46. Delpassand ES, Samarghandi A, Zamanian S, Wolin EM, Hamiditabar M, Espenan GD, et al. Peptide receptor radionuclide therapy with <sup>177</sup>Lu-DOTATATE for patients with somatostatin receptor-expressing neuroendocrine tumors: the first US phase 2 experience. *Pancreas*. 2014; 43: 518-25.
47. Dumont RA, Seiler D, Marincek N, Brunner P, Radojewski P, Rochlitz C, et al. Survival after somatostatin based radiopeptide therapy with <sup>90</sup>Y-DOTATOC

- vs.  $^{90}\text{Y}$ -DOTATOC plus  $^{177}\text{Lu}$ -DOTATOC in metastasized gastrinoma. American journal of nuclear medicine and molecular imaging. 2015; 5: 46-55.
48. Gourni E, Paravatou M, Bouziotis P, Zikos C, Fani M, Xanthopoulos S, et al. Evaluation of a series of new  $^{99\text{m}}\text{Tc}$ -labeled bombesin-like peptides for early cancer detection. Anticancer research. 2006; 26: 435-8.
49. Edge S, Byrd D, Compton C. AJCC Cancer Staging Manual. 7 ed: Springer; 2010.